Title: Mutations in enterobacterial common antigen biosynthesis restore outer membrane barrier function in *Escherichia coli tol-pal* mutants

Authors: Xiang'Er Jiang[a#], Wee Boon Tan[b#], Rahul Shrivastava[a#], Deborah Chwee San Seow[c], Swaine Lin Chen[d,e], Xue Li Guan[c], Shu-Sin Chng[a,b*]

Affiliations:

[a]Department of Chemistry, National University of Singapore, Singapore 117543.

[b]Singapore Center for Environmental Life Sciences Engineering, National University of Singapore (SCELSE-NUS), Singapore 117456.

[c]Lee Kong Chian School of Medicine, Nanyang Technological University, Singapore 636921.

[d]Yong Loo Lin School of Medicine, National University of Singapore, Singapore 119228.

[e]Genome Institute of Singapore, Agency for Science, Technology and Research (A*STAR), Singapore 138672.

[#]These authors contributed equally to the work.

*To whom correspondence should be addressed. E-mail: chmchngs@nus.edu.sg

Keywords: Tol-Pal complex, ECA, MPIase, lipid homeostasis, outer membrane barrier, vancomycin resistance

Important note to readers:

In the previous version of this preprint, we reported that mutations in enterobacterial common antigen (ECA) biosynthesis restore outer membrane (OM) barrier function AND re-establish OM lipid homeostasis in cells lacking the Tol-Pal complex. <u>However, the latter conclusion is no longer correct</u>. Initial experiments to examine OM lipid composition in our strains involved relative quantification of [^{14}C]-acetate-labelled phospholipids (PLs) and lipopolysaccharides (LPS), but the method for LPS quantification (gel separation/phosphor imaging with comparison to standards) was cumbersome and produced rather high variability in the data, especially between different researchers. We have since simplified the experiments by using [^{32}P]-phosphate labelling, allowing quantification of both PLs and LPS using scintillation counting; these changes enabled us to produce robust and consistent data for OM lipid composition analyses. While it is clear that cells lacking the Tol-Pal complex do accumulate excess PLs in the OM (i.e. higher PL/LPS ratio) as previously reported [6], we found that mutations in ECA biosynthesis DO NOT restore lipid homeostasis. Accordingly, we have updated this newer version of the manuscript to reflect the changes in conclusions and discussion.

Summary

The outer membrane (OM) is an essential component of the Gram-negative bacterial envelope that protects cells against external threats. To maintain a functional OM, cells require distinct mechanisms to ensure balance of OM proteins and lipids. Mutations in OM biogenesis and/or homeostasis pathways often result in permeability defects, but how changes in the OM affect barrier function, specifically against large hydrophilic molecules, is unclear. Here, we set out to identify potential mechanism(s) that can alleviate permeability defects in *Escherichia coli* cells lacking the Tol-Pal complex, which accumulate excess PLs in the OM. We identify mutations in enterobacterial common antigen (ECA) biosynthesis that restore OM barrier function but not lipid homeostasis in these strains. Furthermore, we demonstrate that build-up of biosynthetic intermediates, but not loss of ECA itself, contributes to the rescue. This suppression of OM phenotypes is unrelated to known effects resulting from accumulation of ECA intermediates on peptidoglycan. Finally, we reveal that an unusual diacylglycerol pyrophosphoryl-linked lipid species also accumulates in ECA mutants, and might play a role in the rescue phenotype. Our work provides insights into how OM barrier function can be restored independent of lipid homeostasis, and highlights previously unappreciated effects of ECA-related species in OM biology.

52 **Introduction**

53 Gram-negative bacteria are surrounded by a multilayered cell envelope consisting of the inner
54 membrane (IM), the peptidoglycan layer, and the outer membrane (OM). This envelope structure,
55 in particular the OM, plays an essential role in preventing toxic molecules from entering the cell,
56 contributing to intrinsic resistance of Gram-negative bacteria against many antibiotics and
57 detergents [1]. The OM bilayer is asymmetric and has a unique lipid composition, comprising
58 lipopolysaccharides (LPS) in the outer leaflet and phospholipids (PLs) in the inner leaflet. In the
59 presence of divalent cations, LPS molecules in the outer leaflet pack together to form an
60 impervious monolayer [2]; OM structure and lipid asymmetry are thus key determinants for its
61 barrier function. Furthermore, the OM is essential for growth, highlighting the importance of
62 understanding how it is established and maintained.

63 The biogenesis of the OM has been relatively well studied. Key components, including LPS,
64 integral β-barrel proteins, and lipoproteins, are transported and assembled unidirectionally into the
65 OM by the Lpt [3], Bam [4], and Lol machinery [5], respectively. Recently, several systems,
66 including the OmpC-Mla system and the Tol-Pal complex, have been implicated in PL transport
67 between the IM and the OM [6-10]. However, much of bulk PL transport between the two
68 membranes, which occurs in both directions [11-13], is still largely unknown [14]. Nonetheless,
69 an intricate balance between these different OM biogenesis pathways need to be maintained at all
70 times to ensure a stable OM. Such homeostasis of OM components is critical for proper barrier
71 function; yet, we do not fully understand the exact molecular mechanisms of how changes in the
72 OM can translate to permeability defects. In many cases, mutations in OM biogenesis (e.g.

73 *lptD4213, degP, bamB, tol-pal*) result in compromised OM barrier function against both
74 hydrophobic molecules, such as detergents, and even large hydrophilic antibiotics, including
75 vancomycin. One common problem with the OM in these mutants appears to be perturbations in
76 the lipid asymmetry. This give rises to PL bilayer patches that would allow easier diffusive passage
77 of hydrophobic compounds, but not hydrophilic ones. How large hydrophilic drugs like
78 vancomycin cross the OM in mutants with defective OM biogenesis remains elusive.

79 The Tol-Pal complex is a conserved multi-protein system that forms a trans-envelope bridge
80 across the cell envelope in Gram-negative bacteria, and has been known to be generally important
81 for OM stability and integrity [15-17]. It comprises two sub-complexes: TolQRA in the IM and
82 TolB-Pal at the OM. We recently demonstrated that the Tol-Pal complex is involved in the
83 maintenance of OM lipid homeostasis in *Escherichia coli* [6]. Cells lacking the intact complex
84 accumulate excess PLs in the OM, likely due to defects in retrograde (OM-to-IM) PL transport.
85 This increase in PL content may contribute to many known OM permeability/stability phenotypes
86 in *tol-pal* mutants, including hypersensitivity to antibiotics and detergents, leakage of periplasmic
87 content, and OM hypervesiculation [15, 18]. The Tol-Pal complex also plays a key role in cell
88 division; mutant strains lacking functional Tol-Pal exhibits division defects under extreme
89 osmolarity due to incomplete septal cell wall separation and/or improper OM invagination [19,
90 20]. Its role in cell division appears to be independent of its function in OM lipid homeostasis [20].

91 Lipid dyshomeostasis in cells lacking the Tol-Pal complex affects OM barrier function in a
92 way that allows entry of both hydrophobic molecules and large hydrophilic antibiotics. To gain
93 insight(s) into OM lipid homeostasis and how it possibly affects OM function, we asked whether

94 cells lacking the Tol-Pal complex could restore OM barrier function by compensatory mutations
95 in other pathways. We found that disruption in the biosynthesis of enterobacterial common antigen
96 (ECA), a cell surface polysaccharide in the Enterobacteriaceae family [21], rescues OM
97 permeability defects, specifically against vancomycin, in *tol-pal* mutants. Interestingly, in these
98 suppressor mutants, OM lipid homeostasis is still defective even though barrier function is restored.
99 We demonstrated that the rescue requires the accumulation of ECA intermediates, yet is
100 independent of known effects of such build-up on cell wall integrity. Finally, we detected unusual
101 ECA-related lipids in these cells, raising the possibility that they might play a role in restoring OM
102 phenotypes. Our work reveals that the OM barrier, specifically against large hydrophilic molecules,
103 can somehow be re-established even during lipid dyshomeostasis, highlighting the complex and
104 dynamic nature of bacterial OM permeability.

105 **Results**

106

107 **Loss-of-function mutations in ECA biosynthesis rescue OM permeability defects in *tol-pal***

108 **mutants**

109 Cells lacking the Tol-Pal complex have compromised OM integrity due to the accumulation

110 of excess PLs [6]. To gain insight(s) into this phenomenon, we sought to isolate genetic suppressor

111 mutations that could restore OM barrier function in a Δ*tol-pal* mutant. We selected for suppressors

112 that rescue sensitivity to vancomycin, the large cell wall-targeting antibiotic that cannot penetrate

113 an intact and functional OM [22]. Cells have no intrinsic mechanism to alter cell wall structure to

114 give rise to resistance against vancomycin; consistently, suppressor colonies appeared at a low

115 frequency of ~1 x 10^{-9}. We obtained 36 individual suppressor strains, all of which exhibited stable

116 resistance phenotypes against vancomycin similar to a wild-type (WT) strain. We further examined

117 the susceptibilities of these strains against other commonly used antibiotics, including rifampicin

118 and erythromycin. An intact OM also impedes the entry of rifampicin and erythromycin but less

119 effectively than against vancomycin [22]. Eight of the suppressors exhibited near wild-type level

120 resistance against all antibiotics tested (Fig. S1A), thus appearing to have restored OM barrier

121 function. Consistent with this, many of these strains do not leak, or release less, periplasmic RNase

122 I into the media during growth when compared to the parent Δ*tol-pal* mutant (Fig. S1B). We

123 sequenced the genomes of the parent strain and all eight suppressors. Each suppressor strain

124 contains multiple mutations relative to the parent Δ*tol-pal* mutant (Table S1); interestingly, all of

125 these strains have mutations in genes involved in the biosynthesis of ECA (*wecB*, *wecC*, or *wecF*).

126 Six strains contain mutations in *wecC*, which encodes a dehydrogenase enzyme in the ECA
127 synthesis pathway [21, 23]. A 6-bp in-frame insertion in *wecC*, termed *wecC**, is common to four
128 of these strains, suggesting that this allele may be important for restoring OM barrier function in
129 the Δ*tol-pal* mutant. To validate this, we re-constructed the *wecC** mutation in the native locus
130 using a negative selection technique [24] and confirmed that this allele alone is able to rescue
131 vancomycin sensitivity (Fig. 1A) and periplasmic leakiness in Δ*tolQ*, Δ*tolA*, and Δ*tolB* strains (Fig.
132 S2A). The effects of *wecC** on these phenotypes are only partial, however, suggesting that other
133 mutations found in the original suppressor strains may also contribute to restoring OM function.
134 Supporting this idea, the *wecC** mutation does not restore resistance of the *tol-pal* strains against
135 erythromycin and rifampicin (Fig. S2B). Rifampicin (MW ~823) and erythromycin (MW ~734)
136 are much smaller than vancomycin (MW ~1449). It appears that the *wecC** mutation only restores
137 OM barrier function in the *tol-pal* mutant against the passage of larger molecules, including
138 vancomycin and periplasmic proteins (e.g. RNase I).

139 The *wecC** mutation results in the insertion of two amino acids (Pro and Gly) five residues
140 away from the predicted active site Cys in the full-length protein, suggesting that WecC function
141 may be disrupted. Consistent with this, we did not detect any ECA in strains containing this *wecC**
142 allele (Fig. 1C). Furthermore, we showed that deletion of *wecC* also partially restores vancomycin
143 resistance in *tol-pal* strains (Figs. 1B and C). We isolated *wecB* and *wecF* mutations in two of the
144 sequenced suppressor strains (Table S1); we therefore constructed Δ*wecB* and Δ*wecF* mutants to
145 test their rescue phenotypes. Both null mutations partially rescue vancomycin sensitivity in the
146 Δ*tolA* strain (Fig. 1D). We conclude that loss-of-function mutations in ECA biosynthesis likely

147 restore the function of the OM in strains lacking the Tol-Pal complex.

148

149 **Mutations in ECA biosynthesis restore OM barrier function in *tol-pal* strains independent of**

150 **Rcs phosphorelay pathway and/or capsular polysaccharide biosynthesis**

151 Mutations in the ECA pathway are known to trigger the Rcs phosphorelay stress response [25].

152 *tol-pal* mutations also strongly activate the Rcs signaling cascade [26]. Consequently, combined

153 *tol-pal/*ECA mutant colonies exhibit strongly mucoid phenotypes, presumably due to the over-

154 production of capsular polysaccharides (colanic acids), which is regulated by the Rcs pathway [27,

155 28]. We therefore considered whether hyperactivation of the Rcs stress response or up-regulation

156 of colanic acid biosynthesis contributed to the suppression of vancomycin sensitivity by ECA

157 mutations in the *tol-pal* strains. To test this idea, we examined vancomycin sensitivity in *rcsC*

158 (encoding the histidine sensor kinase of the Rcs pathway) [27] or *wcaJ* (encoding the glycosyl

159 transferase that initiates colanic acid biosynthesis) [29] mutants. Deleting *rcsC* or *wcaJ* did not

160 prevent the Δ*wecC* mutation from suppressing vancomycin sensitivity in the Δ*tolA* strain; instead,

161 the Δ*rcsC* Δ*tolA* Δ*wecC* and Δ*wcaJ* Δ*tolA* Δ*wecC* mutants display full resistance against

162 vancomycin, similar to WT cells (Fig. 2A). The mechanism by which the Δ*wecC* mutation

163 suppresses vancomycin sensitivity in *tol-pal* strains is therefore independent of the Rcs

164 phosphorelay and/or colanic acid synthesis. To further demonstrate that the OM barrier function

165 was indeed restored, we showed that a fluorescent analog of vancomycin (BODIPY FL

166 vancomycin) could only penetrate the OM and label peptidoglycan in the Δ*wcaJ* Δ*tolA* strain, but

167 not the Δ*wcaJ* Δ*tolA* Δ*wecC* triple mutant (Fig. 2B). Furthermore, the Δ*wcaJ* Δ*tolA* Δ*wecC* strain

168 also exhibited reduced periplasmic leakiness compared to the Δ*wcaJ* Δ*tolA* mutant (Fig. 2C). We
169 conclude that the Δ*wecC* mutation suppresses OM permeability defects in *tol-pal* strains lacking
170 colanic acid synthesis.

171 We have observed that the Δ*wecC* mutation rescues vancomycin sensitivity in the Δ*tolA* strain;
172 however, we noted that different transductants display varying extents of suppression (Fig. S3).
173 We found that removing RcsC or WcaJ greatly improved the consistency of suppression of the
174 Δ*tolA* phenotype by the Δ*wecC* mutation. This suggests that the initial variability in suppression
175 could be due to varying mucoidal phenotypes. To eliminate this inconsistency, we used strains
176 deleted of *wcaJ* for the rest of this study.

177

178 **Mutations in ECA biosynthesis rescue OM barrier function without restoring lipid**
179 **homeostasis in *tol-pal* mutants**

180 Cells lacking the Tol-Pal complex accumulate excess PLs (relative to LPS) in the OM due to
181 defective retrograde PL transport [6]. Since mutations in the ECA biosynthetic pathway rescue
182 OM defects in *tol-pal* mutants (Fig. 1), we hypothesized that OM lipid homeostasis is restored in
183 these strains. To test this idea, we examined steady state OM lipid compositions in Δ*wcaJ* Δ*tolA*
184 Δ*wecC* mutant cells by measuring the distribution of [^{32}P]-phosphate-labelled PLs between the IM
185 and the OM, and also determining the ratio of PLs to LPS (also labelled with [^{32}P]) in the OM.
186 Consistent with our previous findings, the Δ*tolA* mutant contained more PLs in the OM than WT
187 cells (here in the Δ*wcaJ* background). Specifically, cells lacking TolA accumulate ~1.7-fold excess
188 PLs in the OM (relative to the IM) (Fig. 3A). Furthermore, these cells have ~1.4-fold higher

189 PL/LPS ratio in the OM (Fig. 3B). To our surprise, deleting *wecC* in the Δ*tolA* strain neither re-
190 established intermembrane PL distribution (Fig. 3A), nor restored the OM PL/LPS ratio back to
191 wild-type (Fig. 3B). Consistently, the Δ*tolA* and Δ*tolA* Δ*wecC* strains produced similarly high
192 levels of OM vesicles (Fig. 3C), a phenotype in part attributed to excess PLs in the OM [6]. Even
193 though the OM barrier function (restriction of vancomycin entry and periplasmic RNase I release)
194 has largely been restored (Fig. 2), we conclude that mutations in ECA biosynthesis do not restore
195 OM lipid homeostasis in cells lacking the Tol-Pal complex.
196

197 **Accumulation of ECA intermediates along the biosynthetic pathway is critical for rescue of**
198 **OM barrier function in *tol-pal* strains**

199 The initial steps of ECA biosynthesis involve successive addition of three sugar moieties (*N*-
200 acetyl-D-glucosamine (GlcNAc), *N*-acetyl-D-mannosaminuronic acid (ManNAcA), and 4-
201 acetamido-4,6-dideoxy-D-galactose (Fuc4NAc)) to the undecaprenyl phosphate (und-P) lipid
202 carrier to form Lipid III^{ECA} [21, 30]. After its synthesis at the inner leaflet of the IM, Lipid III^{ECA}
203 is flipped across the membrane by WzxE [31]. This trisaccharide repeating unit is then polymerized
204 by WzyE to form the complete ECA polymer, whose polysaccharide chain length is regulated by
205 WzzE [32, 33]. The whole ECA polymer, which is now carried on undecaprenyl pyrophosphate
206 (und-PP), is finally transferred to form a phosphatidyl-linked species (ECA_{PG}) before being
207 transported to the OM [34-36] (Fig. 4A). The enzymes mediating the last two steps are not known.
208 Of note, a small amount of ECA polymer may be found attached to LPS (ECA_{LPS}) or exists in a
209 soluble cyclic form (ECA_{CYC}) in the periplasm [21]. The production of these two ECA forms is

210 dependent on the LPS O-antigen ligase WaaL and WzzE, respectively [32, 37, 38].

211 We have shown that loss-of-function mutations in *wecB*, *wecC*, and *wecF* rescue vancomycin
212 sensitivity in *tol-pal* mutants (Fig. 1). In the Δ*wcaJ* Δ*tolA* Δ*wecC* strain, we showed that expressing
213 *wecC* in trans reversed the rescue (Fig. S4), indicating that the suppression is solely due to effect(s)
214 arising from the deletion of *wecC*. Mutations in ECA biosynthesis result in both the loss of ECA
215 itself and the build-up of Lipid I^{ECA} or Lipid II^{ECA} intermediates along the pathway (Fig. 4A). To
216 test whether ECA loss is important, we mutated *wecA*, which encodes the enzyme that catalyzes
217 the first committed step in ECA biosynthesis [39]. Interestingly, we found that the Δ*tolA* Δ*wecA*
218 mutant (in the Δ*wcaJ* background) is equally sensitive to vancomycin as the Δ*tolA* mutant (Fig.
219 4B), suggesting that accumulation of intermediates along the ECA pathway, but not the loss of any
220 form of ECA (ECA_{PG}, ECA_{LPS}, or ECA_{CYC}), is responsible for the suppression. Consistent with
221 this idea, removing other ECA biosynthetic enzymes that result in accumulation of intermediates
222 (Lipid I^{ECA} in Δ*wecG*, or Lipid II^{ECA} in Δ*wecE*) fully rescues vancomycin sensitivity in the Δ*tolA*
223 mutant (Fig. 4B). Importantly, rescue of vancomycin sensitivity in these strains was completely
224 abolished when *wecA* was subsequently deleted (Fig. 4C). We conclude that the build-up of Lipid
225 I^{ECA} or Lipid II^{ECA} intermediates can somehow restore OM barrier function in the absence of the
226 Tol-Pal complex.

227 We next tried to test whether mutations in later steps of ECA biosynthesis also suppress *tol-*
228 *pal* phenotypes. However, it has been reported that blocking translocation across the IM or
229 subsequent polymerization of Lipid III^{ECA} causes toxicity in cells. Removing WzxE, together with
230 WzxB, the O-antigen flippase that can also transport Lipid III^{ECA}, is lethal [31] (Fig. S5A). WzyE

231 is also essential for growth [32, 39] (Fig. S5B), precluding further analysis. We therefore turned
232 our attention to WzzE. Remarkably, deletion of *wzzE* partially rescues vancomycin sensitivity in
233 the Δ*tolA* mutant, and this phenotype is dependent on the presence of WecA (Fig. 5A). Cells
234 lacking WzzE are known to lose modality in the ECA polymer, giving rise to a more random
235 distribution of chain lengths [33]. We validated this observation; there are relatively higher levels
236 of shorter chain ECA, presumably including Lipid III^{ECA} precursors, in the Δ*wzzE* mutant (Fig.
237 5B). Taken together, our results suggest that build-up of short-chain or Lipid III^{ECA} intermediates
238 can also possibly rescue OM defects in cells lacking the Tol-Pal complex.

239 It has previously been reported that the terminal GlcNAc moiety attached to the *E. coli* K-12
240 LPS core oligosaccharide is derived from und-PP-GlcNAc (i.e. Lipid I^{ECA}) via the action of WaaL
241 [40, 41]. Since WaaL accepts different und-PP-linked substrates, it may be possible that
242 corresponding modifications of LPS can occur in strains accumulating Lipid II/III^{ECA}; these
243 modified LPS might contribute to restored OM barrier function in the *tol-pal* mutants. To test this
244 idea, we checked if the rescue of vancomycin sensitivity in the Δ*tolA* Δ*wecC* strain is dependent
245 on WaaL. We found that deleting *waaL* did not confer vancomycin sensitivity to the Δ*tolA* Δ*wecC*
246 mutant (Fig. S6), suggesting that the suppression of OM permeability defects is not due to WaaL-
247 dependent LPS modifications.

248

249 **Suppression of OM permeability defects in *tol-pal* strains via accumulation of ECA**
250 **intermediates is independent of und-P sequestration or σ^E and Cpx stress response pathways**

251 Recently, it has been reported that the build-up of ECA "dead-end" intermediates in a strain

252 with defective undecaprenyl pyrophosphate synthase (UppS) [42] can lead to sequestration of und-
253 P, the common precursor for many sugar polymers in the cell envelope including peptidoglycan;
254 this gives rise to severe shape defects such as filamentation and swelling [43]. In our strains that
255 express wild-type UppS and lack colanic acids, we did not observe similarly severe shape defects.
256 Instead, we measured primarily larger cell width in the Δ*wecC* mutant, which were exacerbated in
257 the Δ*tolA* background (Figs. S7A, B). The morphological changes observed in the Δ*tolA* Δ*wecC*
258 strain are thus a combination of defects due to the loss of Tol-Pal function [44], and und-P
259 sequestration caused by accumulation of ECA intermediates [43]. To test whether und-P
260 sequestration contributes to the rescue of vancomycin sensitivity in the Δ*tolA* Δ*wecC* strain, we
261 examined if overexpression of MurA, which can alleviate und-P sequestration effects [43], could
262 reverse the phenotypes. As expected, MurA overexpression was able to fully and partially revert
263 the cell morphological defects in Δ*wecC* and Δ*tolA* Δ*wecC* strains, respectively. However, doing
264 so did not alter vancomycin resistance in the Δ*tolA* Δ*wecC* mutant (Fig. S7C). These data indicate
265 that the effect of accumulation of ECA intermediates in restoring vancomycin resistance in *tol-pal*
266 mutants is independent of und-P sequestration.

267 Accumulation of ECA intermediates, specifically Lipid II^{ECA}, is also known to stimulate the
268 σ^E and Cpx stress response pathways [45]. However, we did not observe significant induction or
269 increased stimulation of σ^E when ECA intermediates were accumulated in WT or Δ*tolA* strains,
270 respectively (Fig. S8A). Removing the Cpx pathway also did not affect vancomycin resistance in
271 the Δ*tolA* Δ*wzzE* strain (Fig. S8B). We conclude that both σ^E and Cpx stress responses are also not
272 involved in the ability of accumulated ECA intermediates to restore the OM barrier function in *tol-*

273 *pal* mutants.

274

275 **Diacylglycerol pyrophosphoryl-linked species also accumulate in ECA biosynthesis mutants**

276 We have shown that accumulation of ECA intermediates rescues vancomycin sensitivity in
277 strains lacking the Tol-Pal complex. However, und-PP-linked intermediates (Lipid I/II/III^{ECA}) may
278 not be the only species accumulated in ECA biosynthesis mutants. In a *Salmonella* Typhimurium
279 Δ*rmlA* mutant, which accumulates Lipid II^{ECA}, a novel diacylglycerol pyrophosphoryl (DAG-PP)-
280 linked species containing the first two sugars of ECA (GlcNAc and ManNAcA) was detected at
281 comparable levels [46]. We therefore sought to determine whether DAG-PP-linked adducts could
282 also be found in our *E. coli* ECA mutants. Using high resolution mass spectrometry (MS), we
283 analyzed lipids extracted from cells lacking WecG, which is expected to accumulate Lipid I^{ECA}.
284 We demonstrated that DAG-PP-GlcNAc species are indeed present in these cells, but not in WT
285 (Figs. 6A, B). Specifically, we detected peaks with m/z values corresponding to DAG-PP-GlcNAc
286 species with various fatty acid compositions in the DAG moiety, namely 32:1 (m/z 928.4927), 34:1
287 (m/z 956.5243), 34:2 (m/z 954.5076), and 36:2 (m/z 982.5391); these are in fact the major DAGs
288 found in native PLs in *E. coli* [47]. Chemical structures of the 32:1 and 34:1 species were assigned
289 and elucidated based on fragmentation patterns in MS/MS (Fig. 7). Furthermore, we showed that
290 the same species were specifically found in the IM but not the OM of the Δ*wecG* mutant, as well
291 as the Δ*wecC* strain (Fig. 6C). It is worth noting that DAG-PP has one extra phosphate moiety and
292 is therefore structurally distinct from phosphatidic acid (i.e. diacylglycerol monophosphate or
293 DAG-P), the final lipid carrier of ECA; instead, the DAG-PP-GlcNAc and DAG-PP-GlcNAc-

294 ManNAc species [46] have been suggested as structural precursors to the MPIase glycolipid [48,
295 49], which is required for protein integration and translocation at the IM. How these DAG-PP-
296 linked species are generated is not fully understood, but their existence highlights the need to
297 consider possible effects of these unusual lipids in our ECA biosynthesis mutants, especially in the
298 context of rescuing OM barrier function in *tol-pal* strains.

299 **Discussion**

300 In this study, we have identified suppressor mutations that can rescue OM permeability defects
301 in cells lacking the Tol-Pal complex, which are known to contain excess PLs in their OM [6, 50].
302 Mutations in ECA biosynthesis restore OM barrier function, thus blocking vancomycin entry and
303 reducing periplasmic leakiness, in *tol-pal* mutant strains (Figs. 1, 2); however, lipid homeostasis
304 was not restored in these strains (Fig. 3). We have demonstrated that these rescue phenotypes are
305 due to the accumulation of intermediate species along the ECA pathway (Figs. 4, 5). Interestingly,
306 aside from the und-PP-linked ECA intermediates, DAG-PP-linked species have also been observed
307 (Figs. 6, 7). How the presence of these ECA-related species could result in the restoration of OM
308 barrier function requires further investigation.

309 The role of ECA in the enterobacterial cell envelope is not known. Strains that do not make
310 ECA are more sensitive to bile salts and produce more OMVs [45, 51]. Loss of cyclic ECA has
311 also been reported to modulate OM function in strains lacking YhdP, a protein of unknown
312 function [38]. These observations suggest that ECA has roles related to the OM. However, we have
313 shown that loss of any form of ECA (ECA_{PG}/ECA_{LPS}/ECA_{CYC}) does not contribute to the
314 restoration of OM barrier function in cells lacking the Tol-Pal complex; instead, the build-up of
315 ECA biosynthetic intermediates is necessary for this rescue. Interestingly, accumulation of und-
316 PP-linked intermediates (in the ECA, O-antigen, and colanic acid pathways) can lead to
317 sequestration of und-P [43, 52], the common lipid carrier also used for peptidoglycan precursors.
318 While this can give rise to morphological changes, the defects were not as severe in our strains
319 (Fig. S5A), which have functional UppS and do not synthesize O-antigens and colanic acids.

320 Overexpression of MurA to alleviate und-P sequestration effects reduced the extent of
321 morphological defects but could not reverse the suppression of *tol-pal* phenotypes (Fig. S5B).
322 Intuitively, weakening the cell wall via und-P sequestration is unlikely to contribute to vancomycin
323 resistance. We therefore believe that restoration of OM phenotypes by ECA intermediates in cells
324 lacking the Tol-Pal complex is independent of und-P sequestration. Furthermore, the rescue
325 mechanism does not appear to involve the major cell envelope stress responses, including Rcs,
326 Cpx, and σ^E pathways (Figs. 2, S8).

327 One possible mechanism where accumulation of und-PP-linked ECA intermediates could
328 affect the physical properties of the OM is via LPS modification. The structure of LPS could affect
329 mechanical strength and barrier function of the OM [53]. In wild-type cells, the full length ECA
330 polymer can be transferred onto LPS core oligosaccharides by WaaL to form ECA_{LPS} [37].
331 However, since deletion of either *wecA* (does not restore OM barrier function) or other *wec* genes
332 (restore OM barrier function) would result in the loss of full length ECA_{LPS}, we ruled out the role
333 of ECA_{LPS} in rescuing the OM permeability defect. It has been reported that the GlcNAc moiety
334 from und-PP-GlcNAc (Lipid I^{ECA}) can itself be transferred onto LPS in a WaaL-dependent manner
335 [40, 41]. We reasoned it is likely that the incomplete sugar subunits on Lipid II/III^{ECA} could also
336 be ligated onto LPS, therefore affecting the physical properties of the OM via LPS modification.
337 However, we showed that deletion of *waaL* in strains that accumulate ECA intermediates did not
338 reverse the suppression of OM permeability defects in the *tol-pal* mutant (Fig. S6). Therefore, the
339 rescue of OM defects by ECA mutations in *tol-pal* strains is unlikely due to WaaL-dependent LPS
340 modifications.

341 While und-PP-linked intermediates are expected to be accumulated in ECA mutants, we and
342 others have also observed the corresponding DAG-PP-linked species [46]. Specifically, DAG-PP-
343 GlcNAc and DAG-PP-GlcNAc-ManNAc species have been detected in strains known to
344 accumulate und-PP-GlcNAc (Lipid I^{ECA}) (Fig. 6) and und-PP-GlcNAc-ManNAc (Lipid II^{ECA}) [46],
345 respectively. Intriguingly, these unusual DAG-PP-linked species have been suggested to be
346 precursors for the membrane protein integrase (MPIase) glycolipid, which in fact has a polymer of
347 9-11 trisaccharide units (identical to the ECA sugars) linked to the DAG-PP carrier [48]. It has
348 been shown that MPIase is important for driving integration of membrane proteins into the IM,
349 and also Sec-dependent translocation of periplasmic and OM proteins across the membrane [48,
350 54]. MPIase biosynthesis has been shown to require the activity of CdsA [49], the CDP-
351 diacylglycerol synthase critical for PL synthesis; however, despite the identical trisaccharide units,
352 this process appears to be independent of the ECA pathway [55]. Consequently, it is not clear how
353 and why DAG-PP-linked species, the presumed precursors to MPIase, would accumulate in ECA
354 biosynthesis mutants. Regardless, we need to consider possible effects of these unusual lipids. We
355 therefore speculate that these DAG-PP-linked species detected in our suppressor strains might
356 somehow modulate the essential membrane protein integration or protein translocation functions
357 of MPIase, possibly affecting a broad spectrum of pathways, and thus indirectly resulting in
358 restored OM barrier function even in the event of lipid dyshomeostasis. The interesting
359 connections between ECA, DAG-PP-linked species, and MPIase, remain to be clarified.

360 Cells lacking the Tol-Pal complex exhibit both cell division and OM stability/permeability
361 defects. The cell division defect, which is more apparent under extreme osmolarity conditions, is

362 thought to be a problem in OM invagination [19] but recently shown to be also related to
363 incomplete septal cell wall separation [20]. The OM defects are largely independent of cell division
364 [20], and likely due to lipid dyshomeostasis, where excess PLs accumulate in the OM [6]. While
365 excess PLs in the OM necessarily affect lipid asymmetry [6] and result in PL bilayer patches that
366 can allow diffusion of hydrophobic molecules, it is unclear how that would increase permeation of
367 large hydrophilic molecules, such as vancomycin and RNase I, across the OM. One possibility is
368 that having more PLs in the OM alters physical properties such as membrane tension and rigidity.
369 These effects could in turn result in the appearance of transient "cracks" in the bilayer, which have
370 been suggested to allow the passage of large hydrophilic compounds [56, 57]. Vancomycin can
371 also cross the OM via the lumen of large porins, if unplugged [22]. Therefore, another possibility
372 is that the changes in lipid composition in the OM of cells lacking the Tol-Pal complex may affect
373 the structure and function of specific large OM porins, causing them to become leaky. How the
374 accumulation of und-PP-linked ECA intermediates and/or DAG-PP-linked species restores OM
375 barrier function against large hydrophilic molecules remains unclear; however, these species might
376 affect other yet-to-be-identified pathways (e.g. MPIase function), possibly indirectly modifying
377 OM physical properties or porin function. The unappreciated roles of ECA-related species in OM
378 biology should be thoroughly investigated.

379 **Experimental Procedures**

380

381 **Strains and growth conditions.** All the strains used in this study are listed in Table S2.
382 *Escherichia coli* strain MC4100 [F^- *araD139* Δ*(argF-lac) U169 rpsL150 relA1 flbB5301 ptsF25*
383 *deoC1 ptsF25 thi*] [58] was used as the wild-type (WT) strain for most of the experiments. NR754,
384 an *araD*$^+$ revertant of MC4100 [59], was used as the WT strain for experiments involving depletion
385 of *wzxE* or *wzyE* from the arabinose-inducible promoter (P_{BAD}). Gene deletion mutants were
386 constructed using recombineering [39, 60] or obtained from the Keio collection [39]. Whenever
387 needed, the antibiotic resistance cassettes were flipped out as described [39, 60]. Gene deletion
388 cassettes were transduced into relevant genetic background strains via P1 transduction [61]. The
389 unmarked and chromosomal *wecC** allele was constructed using a negative selection technique
390 [24]. Luria-Bertani (LB) broth (1% tryptone and 0.5% yeast extract, supplemented with 1% NaCl)
391 and agar were prepared as previously described [61]. When appropriate, kanamycin (kan; 25 μg
392 ml^{-1}), chloramphenicol (cm; 30 μg ml^{-1}), ampicillin (amp; 200 μg ml^{-1}) and spectinomycin (spec;
393 50 μg ml^{-1}) were added.

394

395 **Plasmid construction.** Plasmids used in this study are listed in Table S3. Desired genes were
396 amplified from MC4100 chromosomal DNA using the indicated primers (sequences in Table S4).
397 Amplified products were digested with indicated restriction enzymes (New England Biolabs),
398 which were also used to digest the carrying vector. After ligation, recombinant plasmids were
399 transformed into competent NovaBlue (Novagen) cells and selected on LB plates containing

400 appropriate antibiotics. DNA sequencing (Axil Scientific, Singapore) was used to verify the
401 sequence of the cloned gene.
402
403 **Generation of suppressor mutations and genome sequencing.** To isolate spontaneous
404 suppressor mutants, 10^9 BW25113 Δ*tol-pal*$^{\#}$ cells were plated on LB agar plate supplemented with
405 vancomycin (250 µg/ml) and incubated at 37ºC for 48 h. Individual colonies were picked and
406 restreaked on similar plates to verify their vancomycin resistance properties. 36 separate strains
407 were isolated. To identify the genetic location of mutations, whole genome sequencing was
408 performed. Purified genomic DNA was sheared to approximately 300 bp using a focused
409 ultrasonicator (Covaris). A sequencing library was prepared using the TruSeq DNA PCR Free Kit
410 (Illumina) according to the manufacturer's instructions. This was sequenced using a HiSeq 4000
411 with 2×151 bp reads. Raw FASTQ files were mapped to the *E. coli* W3110 genome sequence
412 (NC_007779.1) using bwa (version 0.7.10) [62]; indel realignment and SNP (single nucleotide
413 polymorphism) calling was performed using Lofreq* (version 2.1.2) with default parameters [63].
414 Resulting variants were assigned to associated genes and amino acid changes using the Genbank
415 Refseq W3110 annotation.
416
417 **Antibiotic sensitivity assay.** Sensitivity against different antibiotics was judged by efficiency of
418 plating (EOP) analyses on LB agar plates containing indicated concentrations of drugs. Briefly, 5-
419 ml cultures were grown (inoculated with overnight cultures at 1:100 dilution) in LB broth at 37˚C
420 until OD_{600} reached ~0.6. Cells were normalized according to OD_{600}, first diluted to OD_{600} = 0.1

421 (≈10^8 cells), and then serially diluted in LB with six 10-fold dilutions using 96-well microtiter
422 plates (Corning). Two microliters of the diluted cultures were manually spotted onto the plates and
423 incubated overnight at 37˚C.
424
425 **RNase I leakage assay.** Measurement of RNase I leakiness was performed using a plate assay as
426 described before [64]. Briefly, 5-ml cultures were grown (inoculated with overnight cultures at
427 1:100 dilution) in LB broth at 37˚C until OD_{600} reached ~0.6. Cells were normalized to OD_{600} =
428 0.001, and 2 µl (≈2,000 cells) were manually spotted onto LB agar plates containing 1.9 mg/ml
429 yeast RNA extract (Sigma). The plates were incubated overnight at 37˚C. To precipitate and
430 visualize RNA, the plates were overlaid with cold (12.5% v/v) trichloroacetic acid.
431
432 **Microscopy.** 5-ml cultures were grown (inoculated with overnight cultures at 1:2000 dilution) in
433 LB broth at 37˚C until OD_{600} reached ~0.5 – 0.6. For FM1-43 (Invitrogen) labelling, 1 µg/ml final
434 concentration of the probe was added to 100 µl of bacterial culture before imaging. For
435 vancomycin-BODIPY FL (Invitrogen) labelling, cell cultures were incubated with 10 µg/ml final
436 concentration of the probe for 15 minutes and washed one time with 1 ml fresh LB before
437 resuspended into 200 µl LB. For all experiments, 5 µl of final cell culture were spotted onto freshly
438 prepared 1% LB agarose pads. Images were acquired using a Zeiss LSM710 confocal microscope
439 at 100x magnification. Cells lengths and widths were measured with Image J [65] and result plotted
440 using the *ggplot2* package in R.
441

442 **σ^E reporter assay.** Strains with plasmid expressing *rpoH*P3::*gfp* or promoterless *gfp* were grown
443 to mid-logarithmic phase ($OD_{600} \approx 0.4$-0.6), then normalized and re-suspended in 150 mM NaCl.
444 Fluorescence level (Ex: 485 nm and Em: 535 nm) of equal amount of cells were measured for each
445 strain using the Victor X4 plate reader (Perkin Elmer). Relative levels of σ^E activation correlates
446 with the expression of GFP due to specific activation of *rpoH*P3 promoter and were determined
447 by normalizing the fluorescence level in strains with *rpoH*P3::*gfp* to the basal fluorescence level
448 in strains expressing *gfp* without promoter. Data from three independent experiments were
449 collected and normalized to the σ^E activation level in WT.
450
451 **Membrane lipid composition analyses.** Experiments to determine steady-state radiolabeled PL
452 distributions in IMs/OMs and PL/LPS ratios in OMs were adapted from methods previously
453 described with some changes [6]. Briefly, 10 ml cultures were grown in LB broth (inoculated from
454 overnight culture to a starting OD_{600} of 0.05) containing [^{32}P]-disodium phosphate (final 1 μCi ml^{-}
455 ^{1}; Perkin Elmer product no. NEX011001MC) until mid-log phase (OD_{600} ~0.5–0.7). Cells were
456 harvested by centrifugation at 4700 × *g* for 10 min, re-suspended in 5 ml of TBS (20 mM pH 8.0
457 Tris-HCl, 150 mM NaCl), and centrifuged again as above. Resulting cell pellets were re-suspended
458 in 5 ml of 20% sucrose in 10mM Tris-HCl pH 8.0 (w/w) containing 1 mM PMSF and 50 μg
459 ml^{-1} DNase I), and lysed by a single passage through a high pressure French press (French Press
460 G-M, Glen Mills) homogenizer at 8000 psi. Unbroken cells were removed by centrifugation at
461 4700 × *g* for 10 min. The cell lysate was collected, and 5.5 ml of cell lysate was layered on top of
462 a two-step sucrose gradient consisting of 40% sucrose solution (5 ml) layered on top of 65%

463 sucrose solution (1.5 ml) at the bottom of the tube. Samples were centrifuged at 36 000 rpm for 16
464 h in a Beckman SW41 rotor in an ultracentrifuge (Model XL-90, Beckman). 0.8-ml fractions
465 (usually 15 fractions) were manually collected from the top of each tube. IM and OM fractions
466 were pooled and diluted with TBS before centrifugation at 36 000 rpm for one hour in the Beckman
467 SW41 rotor to concentrate the membrane. The resulting membrane pellets (not visible) were
468 resuspended in 320 µl TBS for subsequent extraction of PLs (IM) or PLs and LPS (OM). Protocol
469 for the extraction of PLs and LPS had been described previously [6]. Dried PLs were resuspended
470 in 50 µl of a mixture of chloroform:methanol (2:1); while dried LPS pellets were resuspended in
471 50 µl 1% SDS. Equal volumes of PL or LPS solutions were mixed with 2 ml of Ultima Gold
472 scintillation fluid (Perkin Elmer, Singapore) and [^{32}P]-counts were measured using scintillation
473 counting (MicroBeta$^{2®}$, Perkin-Elmer). For each strain, scintillation counts of OM PLs were
474 divided by the total counts of IM PLs and OM PLs to obtain the percentage of OM PLs distribution;
475 while scintillation counts of OM PLs were divided by the counts of OM LPS to obtain the PL/LPS
476 ratio.
477
478 **Quantification of OM vesiculation.** For each strain, 10-ml cells were grown at 37˚C in LB broth
479 (inoculated from an overnight culture at 1:100 dilution) containing [1-^{14}C]-acetate (final 0.2 µCi
480 ml^{-1}; Perkin Elmer product no. NEC084A001MC) until OD600 reached ~0.7. At this OD, cultures
481 were harvested to obtain the cell pellets, and supernatants containing OM vesicles. Cell pellets
482 were washed twice with 10 mM Tris-HCl pH 8.0 and finally suspended in the same buffer (0.2
483 ml). To obtain OM vesicles, supernatants were filtered through 0.45 µm filters followed by

484 ultracentrifugation in a SW41.Ti rotor at 39,000 rpm for 1 h. Finally, the OM vesicles in the
485 resulting pellets were washed and re-suspended in 0.2 ml 10 mM Tris-HCl pH 8.0 buffer.
486 Radioactive counts in cell pellets and OM vesicles were measured after mixing with 2 ml of Ultima
487 Gold scintillation fluid (Perkin Elmer, Singapore). Radioactivity ([^{14}C]-count) was measured on a
488 scintillation counter (MicroBeta$^{2®}$, Perkin-Elmer)
489
490 **Lipid extraction and liquid chromatography-mass spectrometry (LC-MS) analysis.** To
491 prepare the lipid extracts, a modified Bligh and Dyer method was used as described previously
492 [66]. Briefly, bacterial pellets were resuspended in PBS, and chloroform:methanol (1:2, v/v) was
493 added. The mixture was vortexed thoroughly before incubation with shaking at 1,000 rpm, 4°C.
494 Subsequently, water and chloroform were added to each sample to generate a two-phase Bligh-
495 Dyer mixture. The two phases were separated via centrifugation and the lower organic phase was
496 collected in a new tube. The aqueous phase was re-extracted twice with chloroform, and all the
497 organic extracts pooled and dried using a Centrivap and stored at -80°C until use.
498 The lipid samples were reconstituted in chloroform:methanol (1:1, v/v) and analyzed using a
499 high performance chromatography system (1260 Agilent Infinity Quaternary Pump) coupled to an
500 SCIEX QTOF 6600 mass spectrometer in negative electrospray ionization mode. Mass calibration
501 is performed every 5 h, using the automated calibration solution (SCIEX, Canada). For lipid
502 separation, normal phase chromatography was performed as previously described [66]. For
503 characterization of the DAG-PP species using tandem mass spectrometry, multiple collision
504 energies ranging from -55 V to -85 V were used. MS and MS/MS spectra obtained were visualized

505 using Peak View (SCIEX) and graphical representations of the selected peaks of interests were
506 plotted using sigmaplot v10.0.
507
508 **SDS-PAGE and immunoblotting.** SDS-PAGE was performed according to Laemmli using the
509 12% or 15% Tris.HCl gels [67]. For ECA, cell samples were treated with proteinase K (0.25 mg/ml)
510 at 55ºC for 1 h before loading and resolving on 10% Tricine SDS-PAGE gels. Immunoblotting was
511 performed by transferring from the gels onto polyvinylidene fluoride (PVDF) membranes (Immun-
512 Blot® 0.2 µm, Bio-Rad) using the semi-dry electroblotting system (Trans-Blot® TurboTM
513 Transfer System, Bio-Rad). Membranes were blocked using 1X casein blocking buffer (Sigma).
514 Rabbit α-LptE (from Daniel Kahne) was used at 1:5000 dilutions. Rabbit polyclonal α-ECA_{CYC}
515 antisera (generous gift from Jolanta Lukasiewicz), which reacts with all forms of ECA (ECA_{CYC},
516 ECA_{LPS}, ECA_{PG}), was used at 1:800 dilution [68]. Mouse monoclonal α-LPS antibody (against
517 LPS-core) was purchased from Hycult biotechnology and used at 1:5,000 dilutions. α-mouse IgG
518 secondary antibody conjugated to HRP (from sheep) and α-rabbit IgG secondary antibody
519 conjugated to HRP (from donkey) were purchased from GE Healthcare and used at 1:5,000
520 dilutions. Luminata Forte Western HRP Substrate (Merck Milipore) was used to develop the
521 membranes and chemiluminescent signals were visualized by G:BOX Chemi XT 4 (Genesys
522 version1.3.4.0, Syngene).

523 **Acknowledgements**

524 We thank Majid Eshaghi (Genome Institute of Singapore, GIS) for providing σ^E reporter
525 plasmids and Kevin Young (University of Arkansas for Medical Sciences) for the generous gifts
526 of the Δ*wcaJ* strain and the *murA* overexpression plasmid. We are grateful to Jolanta Łukasiewicz
527 (Polish Academy of Sciences) for the α-ECA antibody. WGS work was partially supported by the
528 GIS, and the Singapore Ministry of Health National Medical Research Council
529 (NMRC/CIRG/1357/2013) to S.L.C.. Lipid MS analysis was supported by the Nanyang Assistant
530 Professorship to X.L.G.. All other work were supported by the Singapore Ministry of Education
531 Academic Research Fund Tier 1 Grant, and the Singapore Ministry of Health National Medical
532 Research Council under its Cooperative Basic Research Grant (NMRC/CBRG/0072/2014) to S.-
533 S.C.. The authors declare no conflict of interest.

534

535 **Author contributions**

536 X.E.J., W.B.T., and R.S. performed most of the experiments described in this work; S.L.C.
537 analyzed the whole genome sequencing data of suppressor mutants; D.C.C.S. and X.L.G.
538 performed the MS experiments; S.-S.C. directed and supervised the work; X.E.J., R.S., W.B.T.,
539 and S.-S.C. analyzed the data and wrote the paper; all authors provided critical feedback of the
540 manuscript.

541 **References**

542 1. Nikaido H. Molecular basis of bacterial outer membrane permeability revisited. Microbiol
543 Mol Biol Rev. 2003;67: 593–656.
544 2. Raetz CR, Whitfield C. Lipopolysaccharide endotoxins. Annu Rev Biochem. 2002;71: 635–
545 700.
546 3. Okuda S, Sherman DJ, Silhavy TJ, Ruiz N, Kahne D. Lipopolysaccharide transport and
547 assembly at the outer membrane: the PEZ model. Nat Rev Microbiol. 2016;14: 337–345.
548 4. Hagan CL, Silhavy TJ, Kahne D. β-barrel membrane protein assembly by the Bam complex.
549 Annu Rev Biochem. 2011;80: 189–210.
550 5. Okuda S, Tokuda H. Lipoprotein sorting in bacteria. Annu Rev Microbiol. 2011;65: 239–259.
551 6. Shrivastava R, Xiang'Er J, Chng SS. Outer membrane lipid homeostasis via retrograde
552 phospholipid transport in *Escherichia coli*. Mol Microbiol. 2017;106: 395–408.
553 7. Ekiert DC, Bhabha G, Isom GL, Greenan G, Ovchinnikov S, Henderson IR, Cox JS, Vale RD.
554 Architectures of lipid transport systems for the bacterial outer membrane. Cell. 2017 Apr
555 6;169(2):273-85.
556 8. Ercan B, Low WY, Liu X, Chng SS. Characterization of interactions and phospholipid transfer
557 between substrate binding proteins of the OmpC-mla system. Biochemistry. 2018 Oct
558 4;58(2):114-9.
559 9. Thong S, Ercan B, Torta F, Fong ZY, Wong HY, Wenk MR, Chng SS. Defining key roles for
560 auxiliary proteins in an ABC transporter that maintains bacterial outer membrane lipid
561 asymmetry. Elife. 2016 Aug 16;5:e19042.

562 10. Hughes GW, Hall SC, Laxton CS, Sridhar P, Mahadi AH, Hatton C, Piggot TJ, Wotherspoon
563 PJ, Leney AC, Ward DG, Jamshad M. Evidence for phospholipid export from the bacterial
564 inner membrane by the Mla ABC transport system. Nature Microbiology. 2019
565 Oct;4(10):1692-705.
566 11. Donohue-Rolfe AM, Schaechter M. Translocation of phospholipids from the inner to the outer
567 membrane of Escherichia coli. Proc Natl Acad Sci USA. 1980;77: 1867–1871.
568 12. Jones NC, Osborn MJ. Translocation of phospholipids between the outer and inner membranes
569 of *Salmonella typhimurium*. J Biol Chem. 1977;252: 7405–7412.
570 13. Langley KE, Hawrot E, Kennedy EP. Membrane assembly: movement of phosphatidylserine
571 between the cytoplasmic and outer membranes of *Escherichia coli*. J Bacteriol. 1982;152:
572 1033–1041.
573 14. Shrivastava R, Chng SS. Lipid trafficking across the Gram-negative cell envelope. Journal of
574 Biological Chemistry. 2019 Sep 27;294(39):14175-84.
575 15. Lloubes R, Cascales E, Walburger A, Bouveret E, Lazdunski C, Bernadac A, Journet L. The
576 Tol-Pal proteins of the Escherichia coli cell envelope: an energized system required for outer
577 membrane integrity? Res Microbiol. 2001;152: 523–529.
578 16. Sturgis JN. Organisation and evolution of the *tol-pal* gene cluster. J Mol Microbiol Biotechnol.
579 2001;3: 113–122.
580 17. Cascales E, Gavioli M, Sturgis JN, Lloubes R. Proton motive force drives the interaction of
581 the inner membrane TolA and outer membrane Pal proteins in *Escherichia coli*. Mol
582 Microbiol. 2000;38: 904–915.

583 18. Bernadac A, Gavioli M, Lazzaroni JC, Raina S, Lloubes R. *Escherichia coli tol-pal* mutants
584 form outer membrane vesicles. J Bacteriol. 1998;180: 4872–4878.
585 19. Gerding MA, Ogata Y, Pecora ND, Niki H, de Boer PAJ. The trans-envelope Tol-Pal complex
586 is part of the cell division machinery and required for proper outer-membrane invagination
587 during cell constriction in *E. coli*. Mol Microbiol. 2007;63: 1008–1025.
588 20. Yakhnina AA, Bernhardt TG. The Tol-Pal system is required for peptidoglycan-cleaving
589 enzymes to complete bacterial cell division. Proceedings of the National Academy of
590 Sciences. 2020 Mar 24;117(12):6777-83.
591 21. Kuhn H, Meier-Dieter U, Mayer H. ECA, the enterobacterial common antigen. FEMS
592 Microbiol Lett. 1988;54: 195–222.
593 22. Krishnamoorthy G, Wolloscheck D, Weeks JW, Croft C, Rybenkov VV, Zgurskaya HI.
594 Breaking the permeability barrier of *Escherichia coli* by controlled hyperporination of the
595 outer membrane. Antimicrob Agents Chemother. 2016;60: 7372–7381.
596 23. Meier-Dieter U, Starman R, Barr K, Mayer H, Rick PD. Biosynthesis of enterobacterial
597 common antigen in *Escherichia coli*. Biochemical characterization of *Tn10* insertion mutants
598 defective in enterobacterial common antigen synthesis. J Biol Chem. 1990;265: 13490–13497.
599 24. Khetrapal V, Mehershahi K, Rafee S, Chen S, Lim CL, Chen SL. A set of powerful negative
600 selection systems for unmodified Enterobacteriaceae. Nucleic Acids Res. 2015;43: e83.
601 25. Castelli ME, Véscovi EG. The Rcs signal transduction pathway is triggered by enterobacterial
602 common antigen structure alterations in *Serratia marcescens*. J Bacteriol. 2011;193: 63–74.

603 26. Clavel T, Lazzaroni JC, Vianney A, Portalier R. Expression of the *tolQRA* genes of
604 *Escherichia coli* K-12 is controlled by the RcsC sensor protein involved in capsule synthesis.
605 Mol Microbiol. 1996;19: 19–25.
606 27. Stout V, Gottesman S. RcsB and RcsC: a two-component regulator of capsule synthesis in
607 *Escherichia coli*. J Bacteriol. 1990;172: 659–669.
608 28. Trisler P, Gottesman S. lon transcriptional regulation of genes necessary for capsular
609 polysaccharide synthesis in *Escherichia coli* K-12. J Bacteriol. 1984;160: 184–191.
610 29. Stevenson G, Andrianopoulos K, Hobbs M, Reeves PR. Organization of the *Escherichia coli*
611 K-12 gene cluster responsible for production of the extracellular polysaccharide colanic acid.
612 J Bacteriol. 1996;178: 4885–4893.
613 30. Rahman A, Barr K, Rick PD. Identification of the structural gene for the TDP-Fuc4NAc:lipid
614 II Fuc4NAc transferase involved in synthesis of enterobacterial common antigen in
615 *Escherichia coli* K-12. J Bacteriol. 2001;183: 6509–6516.
616 31. Rick PD, Barr K, Sankaran K, Kajimura J, Rush JS, Waechter CJ. Evidence that the *wzxE*
617 gene of *Escherichia coli* K-12 encodes a protein involved in the transbilayer movement of a
618 trisaccharide-lipid intermediate in the assembly of enterobacterial common antigen. J Biol
619 Chem. 2003;278: 16534–16542.
620 32. Kajimura J, Rahman A, Rick PD. Assembly of cyclic enterobacterial common antigen in
621 *Escherichia coli* K-12. J Bacteriol. 2005;187: 6917–6927.

622 33. Barr K, Klena J, Rick PD. The modality of enterobacterial common antigen polysaccharide
623 chain lengths is regulated by o349 of the *wec* gene cluster of *Escherichia coli* K-12. J
624 Bacteriol. 1999;181: 6564–6568.
625 34. Kuhn HM, Neter E, Mayer H. Modification of the lipid moiety of the enterobacterial common
626 antigen by the "Pseudomonas factor". Infect Immun. 1983;40: 696–700.
627 35. Rinno J, Golecki JR, Mayer H. Localization of enterobacterial common antigen: immunogenic
628 and nonimmunogenic enterobacterial common antigen-containing *Escherichia coli*. J
629 Bacteriol. 1980;141: 814–821.
630 36. Acker G, Bitter-Suermann D, Meier-Dieter U, Peters H, Mayer H. Immunocytochemical
631 localization of enterobacterial common antigen in *Escherichia coli* and *Yersinia enterocolitica*
632 cells. J Bacteriol. 1986;168: 348–356.
633 37. Schmidt G, Mannel D, Mayer H, Whang HY, Neter E. Role of a lipopolysaccharide gene for
634 immunogenicity of the enterobacterial common antigen. J Bacteriol. 1976 May 1;126(2):579-
635 86.
636 38. Mitchell AM, Srikumar T, Silhavy TJ. Cyclic enterobacterial common antigen maintains the
637 outer membrane permeability barrier of *Escherichia coli* in a manner controlled by YhdP.
638 MBio. 2018;9: e01321–18.
639 39. Baba T, Ara T, Hasegawa M, Takai Y, Okumura Y, Baba M, Datsenko KA, Tomita M, Wanner
640 BL, Mori H. Construction of *Escherichia coli* K-12 in-frame, single-gene knockout mutants:
641 the Keio collection. Mol Syst Biol. 2006;2: 2006.0008.

642 40. Feldman MF, Marolda CL, Monteiro MA, Perry MB, Parodi AJ, Valvano MA. The activity
643 of a putative polyisoprenol-linked sugar translocase (Wzx) involved in *Escherichia coli* O
644 antigen assembly is independent of the chemical structure of the O repeat. J Biol Chem. 1999
645 Dec 3;274(49):35129-38.
646 41. Ruan X, Monjarás Feria J, Hamad M, Valvano MA. Escherichia coli and Pseudomonas
647 aeruginosa lipopolysaccharide O-antigen ligases share similar membrane topology and
648 biochemical properties. Mol Microbiol. 2018 Oct;110(1):95-113.
649 42. MacCain WJ, Kannan S, Jameel DZ, Troutman JM, Young KD. A defective undecaprenyl
650 pyrophosphate synthase induces growth and morphological defects that are suppressed by
651 mutations in the isoprenoid pathway of *Escherichia coli*. J Bacteriol. 2018;200: e00255-18.
652 43. Jorgenson MA, Kannan S, Laubacher ME, Young KD. Dead-end intermediates in the
653 enterobacterial common antigen pathway induce morphological defects in *Escherichia coli* by
654 competing for undecaprenyl phosphate. Mol Microbiol. 2016;100: 1–14.
655 44. Rassam P, Long KR, Kaminska R, Williams DJ, Papadakos G, Baumann CG, Kleanthous C.
656 Intermembrane crosstalk drives inner-membrane protein organization in Escherichia coli.
657 Nature communications. 2018 Mar 14;9(1):1-8.
658 45. Danese PN, Oliver GR, Barr K, Bowman GD, Rick PD, Silhavy TJ. Accumulation of the
659 enterobacterial common antigen lipid II biosynthetic intermediate stimulates *degP*
660 transcription in *Escherichia coli*. J Bacteriol. 1998;180: 5875–5884.
661 46. Rick PD, Hubbard GL, Kitaoka M, Nagaki H, Kinoshita T, Dowd S, Simplaceanu V, Ho C.
662 Characterization of the lipid-carrier involved in the synthesis of enterobacterial common

663 antigen (ECA) and identification of a novel phosphoglyceride in a mutant of *Salmonella*
664 *typhimurium* defective in ECA synthesis. Glycobiology. 1998;8: 557–567.
665 47. Oursel D, Loutelier-Bourhis C, Orange N, Chevalier S, Norris V, Lange CM. Lipid
666 composition of membranes of *Escherichia coli* by liquid chromatography/tandem mass
667 spectrometry using negative electrospray ionization. Rapid Commun Mass Spectrom.
668 2018;21: 1721–1728.
669 48. Nishiyama KI, Maeda M, Yanagisawa K, Nagase R, Komura H, Iwashita T, Yamagaki T,
670 Kusumoto S, Tokuda H, Shimamoto K. MPIase is a glycolipozyme essential for membrane
671 protein integration. Nature communications. 2012 Dec 11;3(1):1-0.
672 49. Sawasato K, Sato R, Nishikawa H, Iimura N, Kamemoto Y, Fujikawa K, Yamaguchi T,
673 Kuruma Y, Tamura Y, Endo T, Ueda T. CdsA is involved in biosynthesis of glycolipid MPIase
674 essential for membrane protein integration in vivo. Scientific reports. 2019;9.
675 50. Masilamani R, Cian MB, Dalebroux ZD. *Salmonella* Tol-Pal reduces outer membrane
676 glycerophospholipid levels for envelope homeostasis and survival during bacteremia. Infect
677 Immun. 2018;86: e00173–18.
678 51. McMahon KJ, Castelli ME, Garcia Vescovi E, Feldman MF. Biogenesis of outer membrane
679 vesicles in *Serratia marcescens* is thermoregulated and can be induced by activation of the
680 Rcs phosphorelay system. J Bacteriol. 2012;194: 3241–3249
681 52. Jorgenson MA, Young KD. Interrupting biosynthesis of O antigen or the lipopolysaccharide
682 core produces morphological defects in *Escherichia coli* by sequestering undecaprenyl
683 phosphate. J Bacteriol. 2016;198: 3070–3079.

684 53. Rojas ER, Billings G, Odermatt PD, Auer GK, Zhu L, Miguel A, Chang F, Weibel DB, Theriot
685 JA, Huang KC. The outer membrane is an essential load-bearing element in Gram-negative
686 bacteria. Nature. 2018 Jul;559(7715):617-21.
687 54. Sawasato K, Suzuki S, Nishiyama KI. Increased expression of the bacterial glycolipid MPIase
688 is required for efficient protein translocation across membranes in cold conditions. J Biol
689 Chem. 2019 May 24;294(21):8403-11.
690 55. Kamemoto Y, Funaba N, Kawakami M, Sawasato K, Kanno K, Suzuki S, Nishikawa H, Sato
691 R, Nishiyama KI. Biosynthesis of glycolipid MPIase (membrane protein integrase) is
692 independent of the genes for ECA (enterobacterial common antigen). The Journal of general
693 and applied microbiology. 2019.
694 56. Nikaido H. Restoring permeability barrier function to outer membrane. Chemistry & biology.
695 2005 May 1;12(5):507-9.
696 57. Ruiz N, Wu T, Kahne D, Silhavy TJ. Probing the barrier function of the outer membrane with
697 chemical conditionality. ACS chemical biology. 2006 Jul 7;1(6):385-95.
698 58. Casadaban MJ. Transposition and fusion of the *lac* genes to selected promoters in *Escherichia*
699 *coli* using bacteriophage lambda and Mu. J Mol Biol. 1976;104: 541–555.
700 59. Ruiz N, Gronenberg LS, Kahne D, Silhavy TJ. Identification of two inner-membrane proteins
701 required for the transport of lipopolysaccharide to the outer membrane of *Escherichia coli*.
702 Proc Natl Acad Sci USA. 2008;105: 5537–5542.

703 60. Datsenko KA, Wanner BL. One-step inactivation of chromosomal genes in Escherichia coli
704 K-12 using PCR products. Proceedings of the National Academy of Sciences. 2000 Jun
705 6;97(12):6640-5.
706 61. Silhavy TJ, Berman ML, Enquist LW. Experiments with Gene fusions. New York: Cold
707 Spring Harbor Laboratory; 1984.
708 62. Li H, Durbin R. Fast and accurate short read alignment with Burrows-Wheeler Transform.
709 Bioinformatics. 2009;25: 1754–60.
710 63. Wilm A, Aw PP, Bertland D, Yeo GH, Ong SH, Wong CH, Khor CC, Petric R, Hibberd ML,
711 Nagarajan N. LoFreq: a sequence-quality aware, ultra-sensitive variant caller for uncovering
712 cell-population heterogeneity from high-throughput sequencing datasets. Nucleic Acids Res.
713 2012;40: 11189–11201.
714 64. Lazzaroni JC, Portalier RC. Isolation and preliminary characterization of periplasmic-leaky
715 mutants of *Escherichia coli* K-12. FEMS Microbiol Lett. 1979;5: 411–416.
716 65. Schneider CA, Rasband WS, Eliceiri KW. NIH image to ImageJ: 25 years of image analysis.
717 Nat methods. 2012;9: 671–675.
718 66. Guan XL, Mäser P. Comparative sphingolipidomics of disease-causing trypanosomatids rveal
719 unique lifecycle- and taxonomy-specific lipid chemistries. Sci Rep. 2017;7: 13617.
720 67. Laemmli UK. Cleavage of structural proteins during the assembly of the head of
721 bacteriophage T4. Nature. 1970;227: 680–685.

722 68. Gozdzlewicz TK, Lugowski C, Lukasiewicz J. First evidence for a covalent linkage between
723 enterobacterial common antigen and lipopolysaccharide in *Shigella sonnei* phase II ECALPS.
724 J Biol Chem. 2014;289: 2745–2754.
725 69. Raivio TL, Popkin DL, Silhavy TJ. The Cpx envelope stress response is controlled by
726 amplification and feedback inhibition. J Bacteriol. 1999;181: 5263–5272.
727 70. Cherepanov PP, Wackernagel W. Gene disruption in Escherichia coli: TcR and KmR cassettes
728 with the option of Flp catalyzed excision of the antibiotic-resistance determinant. Gene.
729 1995;158: 9–14.

730 **Figures**

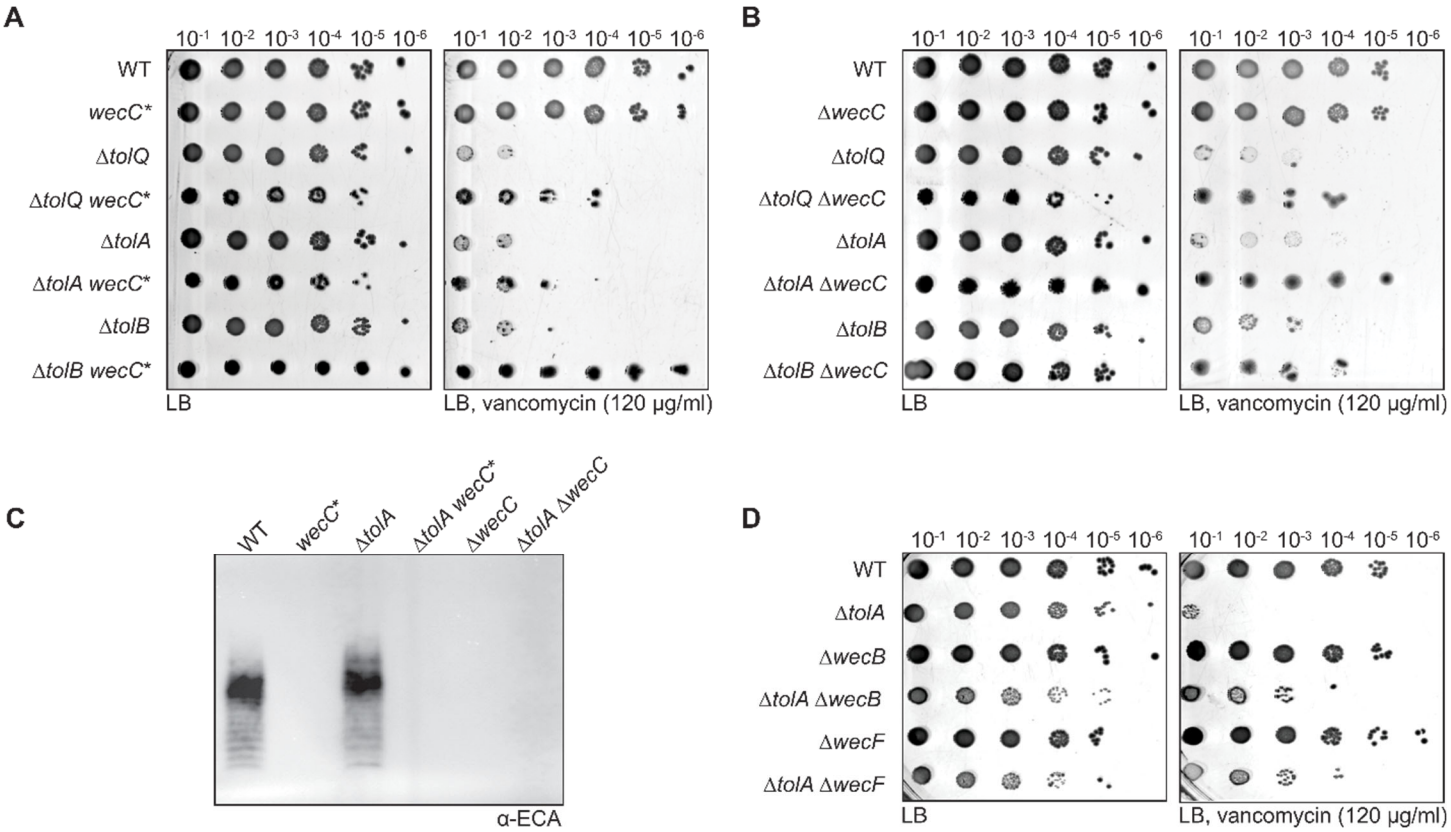

731

732 **Fig. 1** Loss-of-function mutations in the ECA pathway rescue vancomycin sensitivity in *tol-pal*
733 mutants. Vancomycin sensitivity of indicated *tol-pal* strains with or without (A) *wecC**, (B)
734 Δ*wecC*, and (D) Δ*wecB*/Δ*wecF* mutations based on efficiency of plating (EOP) on LB agar plates
735 supplemented with vancomycin (120 µg/ml). (C) ECA levels in wild-type (WT) and Δ*tolA* strains
736 with or without *wecC** and Δ*wecC* mutations as judged by immunoblot analysis using α-ECA
737 antibody. Samples were normalized by OD_{600} and treated with proteinase K prior to Tricine SDS-
738 PAGE/immunoblotting.

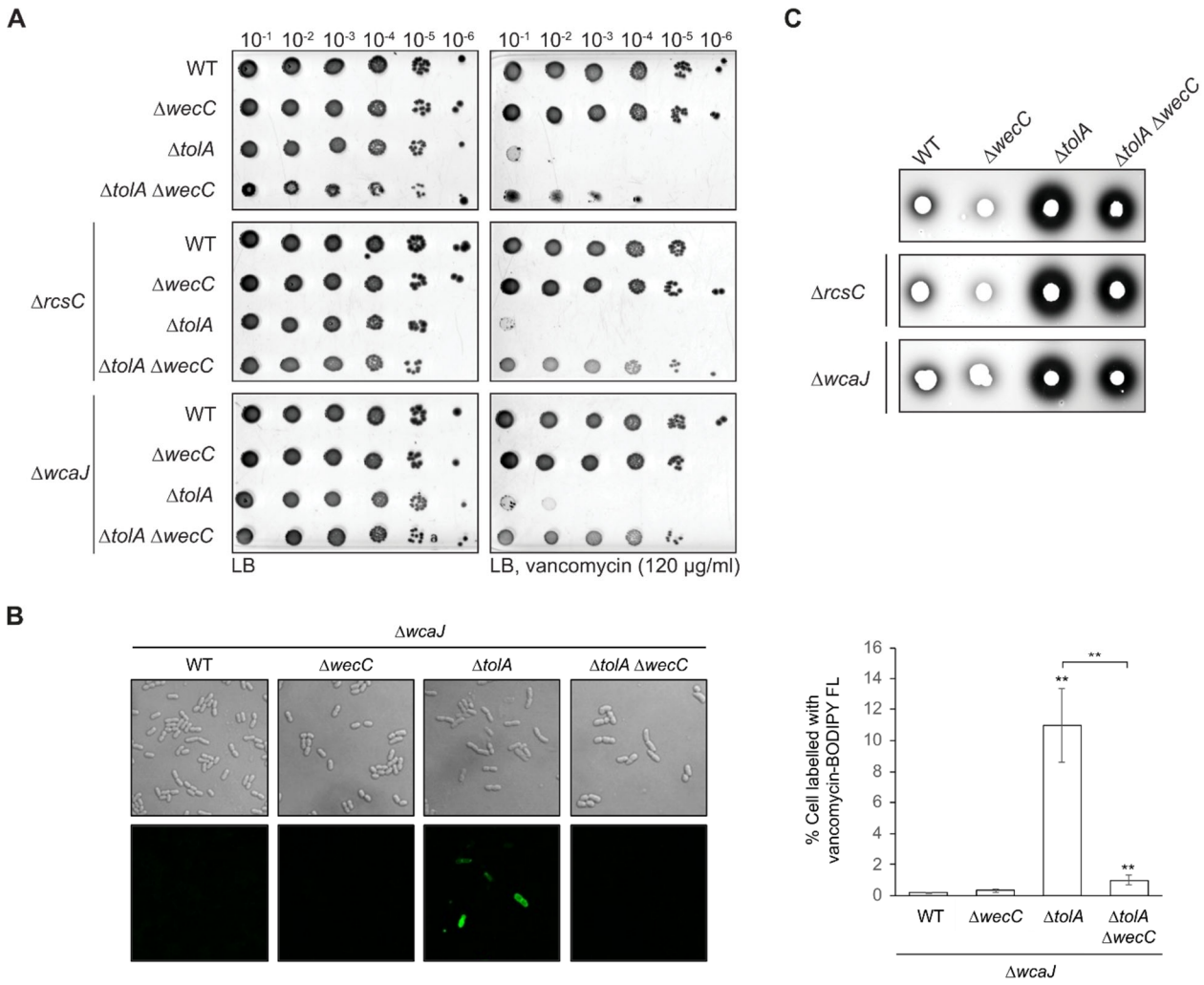

Fig. 2 Restoration of OM permeability defects by Δ*wecC* in cells lacking TolA does not require the Rcs phosphorelay cascade and/or capsular polysaccharide biosynthesis. (A) Vancomycin sensitivity of indicated strains in either Δ*rcsC* or Δ*wcaJ* backgrounds based on EOP on LB agar plates supplemented with vancomycin (120 µg/ml). (B) RNase I leakage in the same strains as (A), as judged by RNA degradation (halo formation) around cells spotted on LB agar plates containing yeast RNA, subsequently precipitated with trichloroacetic acid. (C) Confocal microscopy images of indicated strains (Δ*wcaJ* background) after incubation with BODIPY FL vancomycin. (Right) Quantification of the percentage of cells circumferentially labelled with BODIPY FL vancomycin

748 from different field of view (n = 6); error bars represent standard deviation. Student's t-tests: **,

749 $p < 0.005$ (as compared to WT, unless otherwise indicated).

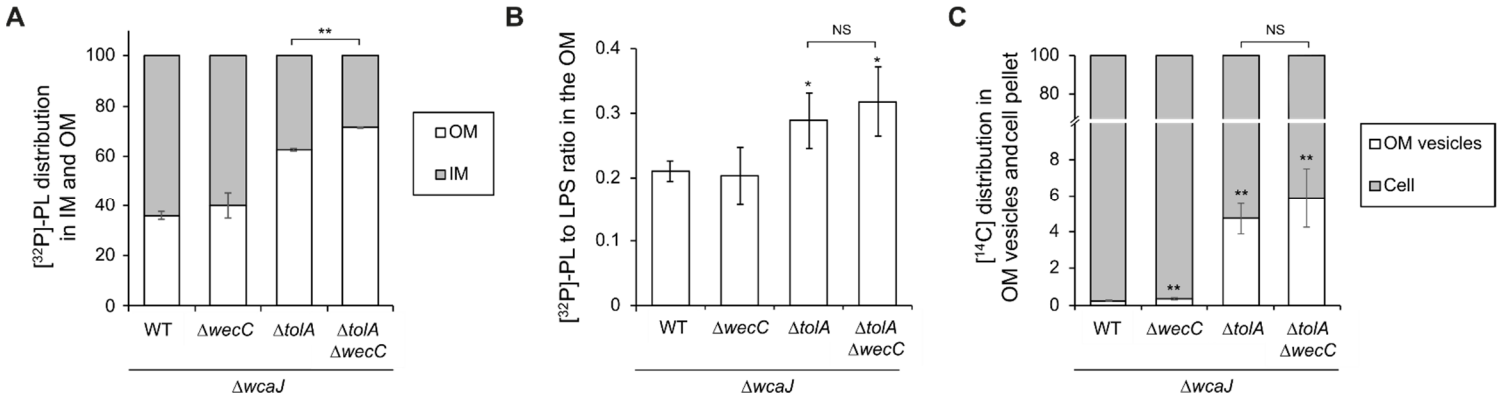

Fig. 3 Δ*wecC* mutation does not restore OM lipid homeostasis in cells lacking TolA. (A) Steady-state [^{32}P]-labelled PL distribution profiles of indicated Δ*wcaJ* strains. Cells were grown in the presence of [^{32}P]-phosphate to label PLs in the IMs and OMs. [^{32}P]-scintillation counts detected in PLs extracted from IM and OM fractions were expressed as a percentage of their sums, averaged across three replicate experiments. (B) Steady-state PL:LPS ([^{32}P]-phosphate labelled) ratios in the OMs of indicated Δ*wcaJ* strains. Arbitrary OM PL:LPS ratios were calculated based on [^{32}P]-scintillation counts detected from PL or LPS, differentially extracted from the OM fractions of the indicated strains. (C) Steady-state distribution of [^{14}C]-acetate-labelled lipids found associated with cells (total membranes) or OM vesicles for the indicated strains. Error bars represent standard deviations calculated from triplicate experiments. Student's t-tests: $*$, $p < 0.05$; $**$, $p < 0.005$; NS, not significant (as compared to WT, unless otherwise indicated).

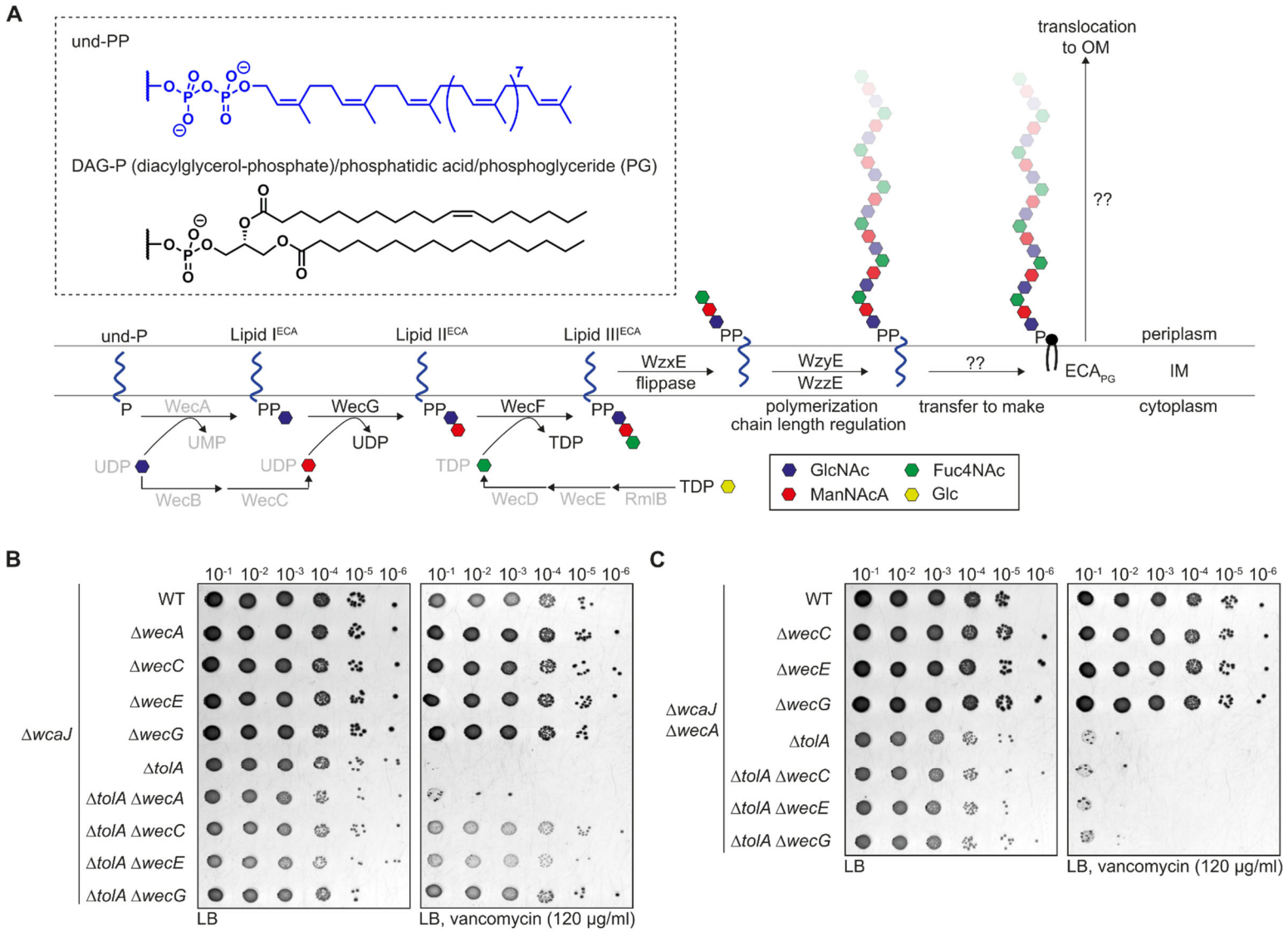

Fig. 4 Accumulation of ECA biosynthetic intermediates restores vancomycin resistance in cells lacking TolA. (A) Schematic of the ECA biosynthetic pathway illustrating und-PP-GlcNAc-ManNAcA-Fuc4NAc (Lipid III^{ECA}) synthesis at the inner leaflet of IM, and subsequent polymerization at the outer leaflet. The final ECA polymer (ECA_{PG}) is attached to a phosphoglyceride (i.e. diacylglycerol-phosphate (DAG-P) aka phosphatidic acid) and transported to the OM. Chemical structures of und-PP and DAG-P anchors are shown. (B, C) Vancomycin sensitivity of the Δ*wcaJ* Δ*tolA* strain with or without indicated *wec* mutations in otherwise (B) WT

769 or (C) Δ*wecA* backgrounds, based on efficiency of plating (EOP) on LB agar plates supplemented

770 with vancomycin (120 ug/ml).

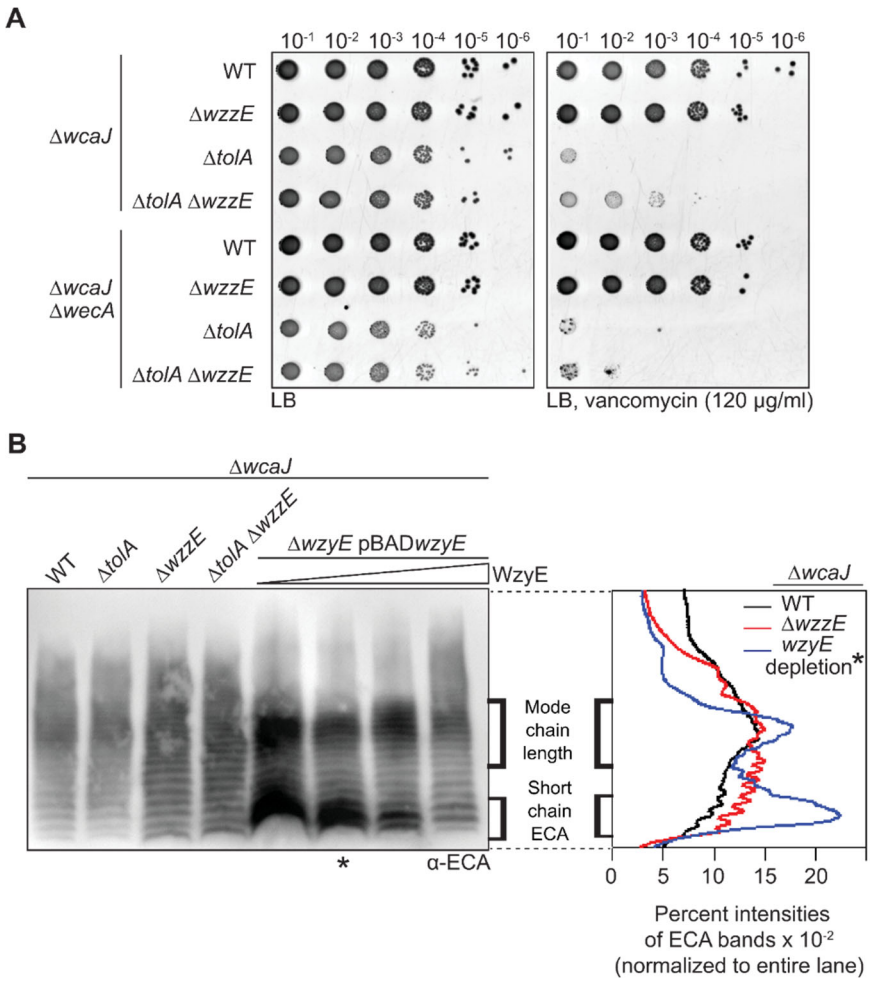

Fig. 5 Partial accumulation of Lipid III^{ECA} and/or short chain ECA rescues vancomycin sensitivity in cells lacking TolA. (A) Vancomycin sensitivity of the Δ*wcaJ* Δ*tolA* strain with or without Δ*wzzE* mutation in otherwise WT or Δ*wecA* backgrounds, based on efficiency of plating (EOP) on LB agar plates supplemented with vancomycin (120 ug/ml). (B) ECA profiles in the indicated Δ*wcaJ* strains as judged by immunoblot analysis using α-ECA antibody. Samples were normalized by OD_{600} and treated with proteinase K prior to Tricine SDS-PAGE/immunoblotting. Profiles in strains progressively depleted of *wzyE* are used to visualize accumulation of Lipid III^{ECA}. Relative band intensities from ECA profiles of WT, Δ*wzzE,* and *wzyE*-depleted (*) strains are shown on the right.

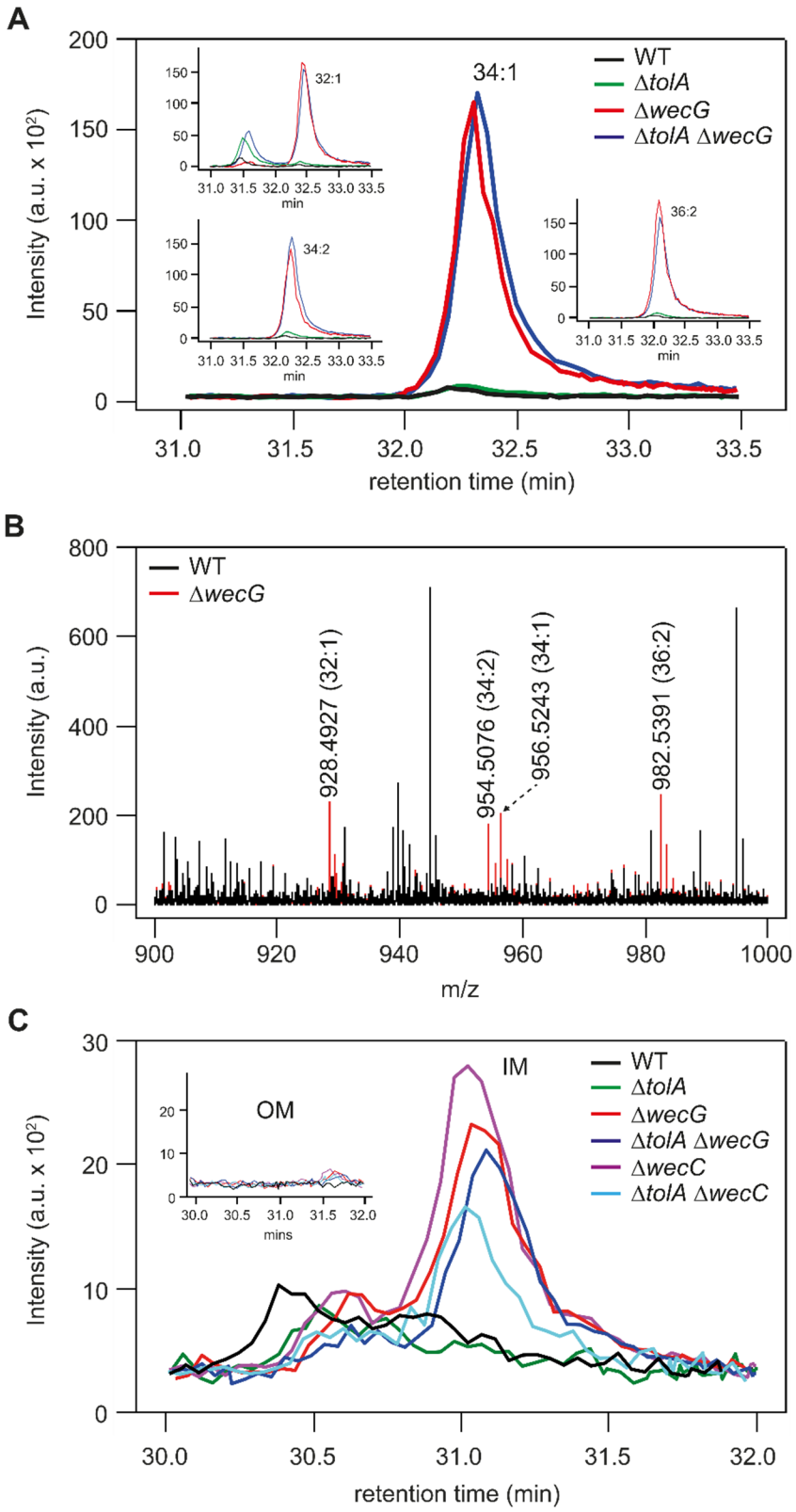
A
Intensity (a.u. x 10²)
retention time (min)
34:1
32:1
34:2
36:2
min
WT
ΔtolA
ΔwecG
ΔtolA ΔwecG
B
Intensity (a.u.)
m/z
WT
ΔwecG
928.4927 (32:1)
954.5076 (34:2)
956.5243 (34:1)
982.5391 (36:2)
C
Intensity (a.u. x 10²)
retention time (min)
IM
OM
mins
WT
ΔtolA
ΔwecG
ΔtolA ΔwecG
ΔwecC
ΔtolA ΔwecC

780

781 **Fig. 6** Strains lacking WecG or WecC accumulate DAG-PP-GlcNAc species in the IM. (A) Ion
782 chromatogram (XIC) of 34:1 DAG-PP-GlcNAc (m/z 956.5243) extracted from LC-MS analyses
783 of total lipids isolated from indicated Δ*wcaJ* strains. Inset, XICs of corresponding 32:1 (m/z
784 928.4927), 34:2 (954.5076) and 36:1 (m/z 982.5391) species. (B) Mass spectra obtained from
785 integration of XIC peak region in (A) of Δ*wcaJ* (WT) and Δ*wcaJ* Δ*wecG* strains. WT peaks (black)
786 are overlaid on top of Δ*wecG* peaks (red), illustrating unique DAG-PP-GlcNAc signals in the latter
787 strain. (C) XICs of 34:1 DAG-PP-GlcNAc (m/z 956.5243) extracted from LC-MS analyses of IM
788 lipids isolated from indicated Δ*wcaJ* strains. Inset, XICs of the same species from OM lipids.

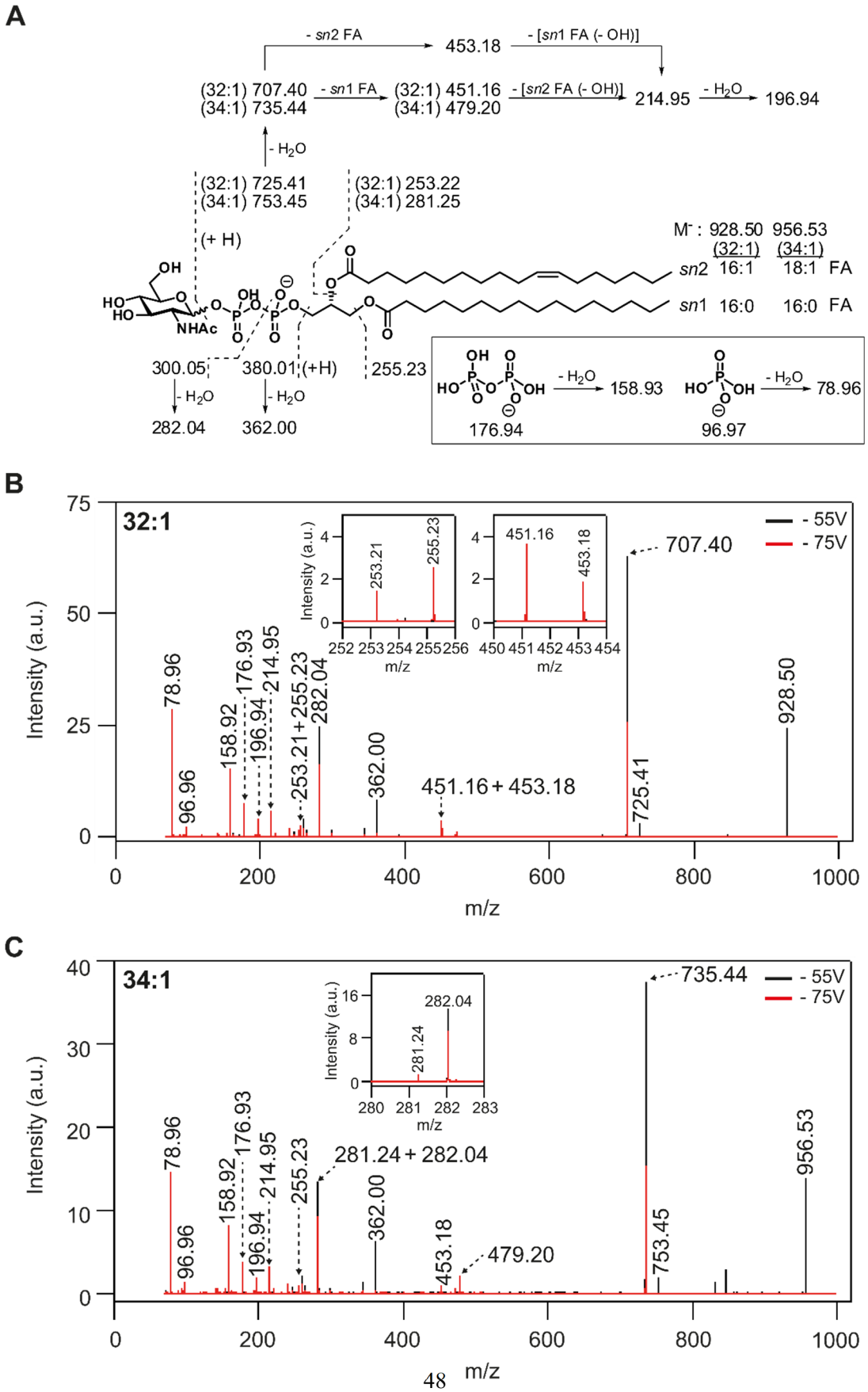
A
- sn2 FA
453.18
- [sn1 FA (- OH)]
(32:1) 707.40
(34:1) 735.44
- sn1 FA
(32:1) 451.16
(34:1) 479.20
- [sn2 FA (- OH)]
214.95
- H2O
196.94
- H2O
(32:1) 725.41
(34:1) 753.45
(32:1) 253.22
(34:1) 281.25
(+ H)
M- : 928.50 956.53
(32:1) (34:1)
sn2 16:1 18:1 FA
sn1 16:0 16:0 FA
300.05
380.01 (+H)
255.23
- H2O
282.04
- H2O
362.00
176.94
- H2O
158.93
96.97
- H2O
78.96
B
32:1
- 55V
- 75V
Intensity (a.u.)
m/z
707.40
928.50
725.41
451.16 + 453.18
362.00
253.21 + 255.23
282.04
214.95
196.94
176.93
158.92
96.96
78.96
C
34:1
- 55V
- 75V
735.44
956.53
753.45
479.20
453.18
362.00
255.23
281.24 + 282.04
281.24
282.04

790 **Fig. 7** The chemical structures of DAG-PP-GlcNAc species are deduced from MS fragmentation
791 analysis. (A) Proposed fragmentation pattern with mass assignments of 32:1 and 34:1 DAG-PP-
792 GlcNAc species. (B and C) MS/MS spectra of (B) 32:1 and (C) 34:1 DAG-PP-GlcNAc species at
793 indicated collision energies. Spectrum at high collision energy (-75 V, red) is overlaid on top of
794 that at low collision energy (-55 V, black).